

# ENHANCED PREDNISONONE REMOVAL BY CATALYTIC WET AIR OXIDATION USING SEWAGE SLUDGE DERIVED CATALYST

Diego Huber-Benito<sup>\*</sup>, Maria Martin-Martinez, Marcos Larriba, Ismael Águeda, Juan García

Catalysis and Separation Processes Group (CyPS), Chemical Engineering and Materials Department, Faculty of Chemistry, Complutense University of Madrid, Avda. Complutense s/n, 28040 Madrid, Spain.

dihuber@ucm.es

## Abstract

Sewage sludge-based catalysts have been used for the first time for the catalytic wet-air oxidation (CWAO) of prednisone, a glucocorticoid pharmaceutical pollutant present in various aquatic environmental matrices. This research focuses on transforming dry sludge into carbonaceous catalysts through pyrolysis and post-treatment. Various parameters have been considered for the synthesis, finding that pyrolysis temperature and acid washing are determinant for specific surface area development. The sewage sludge derived catalysts exhibit high catalytic activity in the CWAO of prednisone ( $D_{\text{cat}} = 0.3 \text{ g}\cdot\text{L}^{-1}$ ,  $T = 100 \text{ }^\circ\text{C}$ ,  $P = 15 \text{ bar}$ ). The development of porosity enhances their catalytic properties, the C-750-N catalysts demonstrated the highest activity for prednisone with 66% TOC reduction, initial reaction rate  $0.0092 \text{ mg}\cdot\text{s}^{-1}$  and 66%  $\text{CO}_2$  selectivity. The study provides valuable insights into the synthesis, characterization, and application of sewage sludge-derived catalysts, offering a sustainable solution for wastewater treatment and pharmaceutical pollutant removal. Our present study indicates that catalysts with unique reforming properties may be potentially applicable for prednisone treatment and industrial applications.

**Keywords**— Sewage sludge derived catalyst, Prednisone, Catalytic wet air oxidation, Degradation mechanism

## 1. Introduction

Sewage sludge is a byproduct of water treatment which receives significant attention. Over 9.8 million tons are produced annually in Europe [1], and it has been predicted that its generation will increase up to 2% by volume annually. Many countries have restricted the disposal of sewage sludge by landfilling, fertilising, composting or incineration due to environmental concerns, so new proposals are needed to valorise this residue [2]. Both landfilling and composting have the potential to disperse undesired pathogens. The use of sewage sludge as a fertilizer is limited due to its high metal content. In relation to incineration, this technique can be challenging due to the high amount of sludge with high volatile content [3]. Recently, biomass materials have become the preferred raw materials for producing activated carbons thanks to their favourable qualities, such as a wealth of functional groups, a well-developed pore structure and the existence of abundant reserves [4]. Thanks to the high proportion of carbon, iron, silicon and other metals, sewage sludge can be used as precursor for the production of efficient carbonaceous catalysts. For example it has been used for removal of phenolic compounds [5, 6].

---

<sup>\*</sup>Corresponding

Different methods can be used for the synthesis of Sewage Based Catalysts (SBCs), specifically pyrolysis, microwave digestion and hydrothermal treatment, being pyrolysis the most commonly used method [7]. Various parameters in the pyrolysis can change the quality attributes of the produced biochar, nevertheless pyrolysis temperature is the most influential on biochar properties like specific surface area or acid-base properties of the surface [8]. Elevated pyrolysis temperatures lead to reduced biochar yield, diminished total nitrogen content, decreased water sorption capacity, and cation exchange capacity (CEC). Conversely, it raises the biochar's pH, specific surface area, carbon content, available nutrients, and stability of the heavy metals. Thus, the ideal pyrolysis temperature must be modulated depending on the future application of the SBC [9].

On the other hand, Emerging Pollutants (EPs) include a diverse variety of synthetic chemicals (such as cosmetics, pesticides, personal and household care products, pharmaceuticals, among others) that are globally utilized [10]. Pharmaceutical active compounds are some of the most critical emerging pollutants nowadays. Their appearance in the aquatic environment followed by a chronic exposure can cause significant damage to the aquatic ecosystem [11]. Between the different types of pharmaceutical emerging pollutants, there is a recent focus on anticancer drugs. The International Agency for Research on Cancer estimated that in the year 2020, approximately 18.1 million new cases of cancer were diagnosed worldwide. It is projected that the number of new cases will increase in the next two decades to 28 million new cases per year by 2040. The growing use of anticancer treatments joined to the high excretion rate, has led to the presence of cytostatic drugs in the environment [12]. These compounds have been detected in wastewaters at extremely low concentrations ranging from  $\text{mg}\cdot\text{L}^{-1}$  in hospital wastewaters to  $\text{ng}\cdot\text{L}^{-1}$  in urban wastewaters [13].

Among these compounds, prednisone is a glucocorticoid pollutant highly used due to its anti-inflammatory effect [14]. It has been shown to have an endocrine disrupting effect in aquatic media [15], and the continuous exposure to this compound has negative effects on crustacean life [14]. In addition, it is considered as an anticancer drug with a higher predicted environmental concentration (PEC) than others in Spain [16]. Glucocorticoids have also been detected in surface water, wastewater and hospital wastewater in China, Spain, Japan, and France [17].

In the context of treating pollutants in aqueous effluents, a non-destructive technique like adsorption, filtration or extraction is usually used as a preliminary concentration step before the chemical destruction of the pollutant. Adsorption is a highly efficient technique for a wide spectrum of organic pollutants. It is widely recognized that activated carbon possesses a substantial surface area and can adsorb considerable amounts of pollutants [18]. Membrane filtration involves the use of a membrane to separate the solute from the water as it flows through [19]. Solvent extraction is another technique which is based on using the distribution coefficient between two immiscible liquid phases [20].

Alternatively, among the destructive methods, the predominant strategy for waters typically involves a traditional biological treatment. Nevertheless, it becomes unfeasible to employ this approach for streams characterized by elevated levels of organic matter and/or bio-toxic substances [21]. In these cases, where conventional treatments are ineffective, numerous alternative options exist. Incineration can provide nearly complete pollutant removal, but with significantly high energy expenses and an organic load exceeding 25% to ensure self-sustaining oxidation [21]. Another option is the supercritical wet air oxidation (SWAO), a technique that works above the critical point of water, at operating conditions of 500-650 °C and 250-300 bar, with reactor residence times under a minute [22]. Compared to the incineration and the supercritical wet air oxidation, catalytic wet air oxidation (CWAO) might further be considered as an energy-saving catalytic method. Temperature and pressure parameters in CWAO process oscillate between 100-200 °C and 5-30 bar. CWAO generates highly reactive hydroxyl radicals through the decomposition of oxygen, enabling the efficient degradation of resilient organic pollutant molecules [23]. Nevertheless, the primary drawback is the ongoing challenge of developing cost-effective, active, selective, and stable catalytic materials, particularly for applications requiring substantial treatment capacity [24].

In CWAO technology, heterogeneous catalysts are employed, and the selection of supports holds significant importance. Typical supports include metal oxides like  $\text{Al}_2\text{O}_3$  and  $\text{TiO}_2$ , activated carbon, and molecular sieves [25]. Among these options, activated carbon stands out as a frequently chosen catalyst support due to its extensive surface area [26]. Despite the wide range of synthesis methods, SBCs have proven to be effective in CWAO. Chemical activation with  $\text{FeCl}_3\cdot 6\text{H}_2\text{O}$  was employed to prepare a SBC used to remove ciprofloxacin [27], while activation with  $\text{FeSO}_4$  was used for the synthesis of a catalyst used for the oxidation of 2-chlorophenol [28]. In addition, a physical activation synthesis with  $\text{CO}_2$  and  $\text{H}_2\text{O}$  was tested for the treatment of phenolic waters [29, 30].

The present work aims the upgrading of urban sewage sludge into a catalyst for the removal of prednisone by CWAO. Different pyrolysis conditions and atmospheres were tested in the catalysts synthesis. Furthermore, a post-treatment with nitric and hydrochloric acid at different temperatures and potassium permanganate was

made to improve the catalytic properties of the obtained material. The post-treatment was conducted to develop the specific surface area or increase functional activity groups on the surface of the catalyst. To our knowledge, the removal by CWAO of this emerging micro-pollutant has not been previously reported in the literature. Therefore, there is a significant knowledge gap in the application of cheaper based catalysts sewage sludge-derived carbon materials for the removal of emerging pharmaceutical compounds from wastewater effluents by CWAO.

## 2. Materials and Methods

### 2.1. Materials

Prednisone ( $\geq 98\%$ ) was obtained by Sigma Aldrich. High pressure liquid chromatography (HPLC) analysis were performed with acetonitrile ( $\geq 98\%$ ) for HPLC analysis supplied by Sigma Aldrich and acetic acid with a purity of 99.7% provided by Panreac. For the catalyst synthesis, Labkern provided nitric acid (65%) and hydrochloric acid (37%), while Probus supplied potassium permanganate ( $\geq 99\%$ ). All gases used in the studies were of 3X purity supplied by Nippon Gases. Synthetic air was used for the oxidation experiments, while carbon dioxide and nitrogen were used for the catalyst synthesis.

### 2.2. Catalyst preparation

#### 2.2.1. Pyrolysis

The sewage sludge was obtained from an urban waste water treatment plant (WWTP) located in Segovia, Spain. The sewage sludge was dried at 105 °C and grounded to powder. The pyrolysis was carried out in a horizontal quartz furnace. A ramp temperature of 5 °C·min<sup>-1</sup> was applied to all the synthesis with an isotherm of 2 hours and 30 minutes. Atmospheres of CO<sub>2</sub> or N<sub>2</sub> have been tested, in addition to different pyrolysis temperatures (600-850 °C). As for the nomenclature of the samples, the first letter indicates the atmosphere used, 'C' for CO<sub>2</sub> and 'N' for N<sub>2</sub>, and the following number indicates the temperature of the pyrolysis process.

#### 2.2.2. Post-treatment

A post-treatment was done with different agents under different conditions to observe the effects on the catalytic properties. Nitric acid at 80 °C, nitric acid and hydrochloric acid at room temperature, potassium permanganate at 80 °C and room temperature were used in addition to the no-treated material. Nitric acid was used at 7M concentration, hydrochloric acid at 1M and permanganate at the solubility limit of the salt in water. All the agents were used in a solid solution ratio of 1 g·10 mL<sup>-1</sup>. Finally, the obtained material was filtered and rinsed with distilled water to constant pH. The samples washed with nitric acid were labelled with an 'N' at the end of their name, while the sample washed with hydrochloric acid were labelled with 'Cl' and potassium permanganate with 'P'. If post-treatment involved temperature, the specific temperature applied was also introduced. Figure 1 show a detailed diagram of the synthesis steps, and Table 1 provides a summary of the synthesised catalysts.

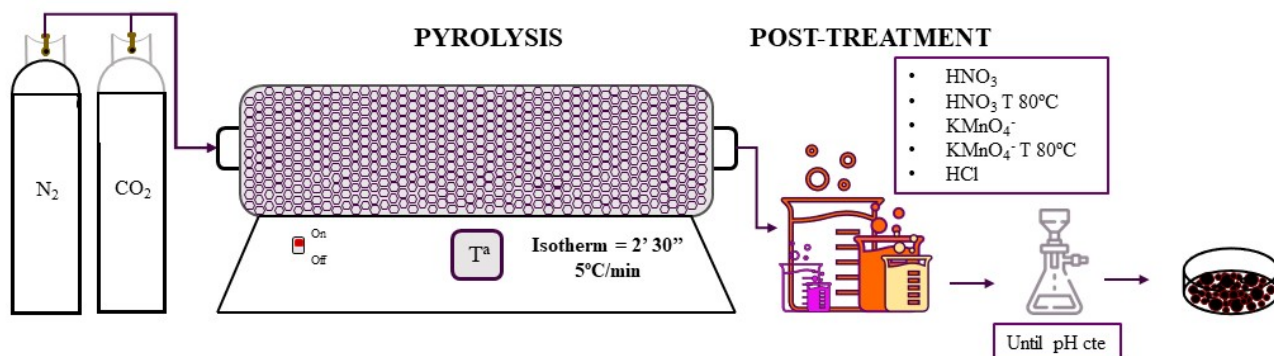


Figure 1: Experimental procedure for the synthesis of the different catalysts from sewage sludge.

Table 1: Summary of catalysts synthesised using different agents and conditions.

Catalyst	Preparation
N-600	Pyrolysis conducted in a N <sub>2</sub> atmosphere at 600 °C.
C-600	Pyrolysis conducted in a CO <sub>2</sub> atmosphere at 600 °C.
N-750	Pyrolysis conducted in a N <sub>2</sub> atmosphere at 750 °C.
C-750	Pyrolysis conducted in a CO <sub>2</sub> atmosphere at 750 °C.
C-750-N-80	Pyrolysis conducted in a CO <sub>2</sub> atmosphere at 750 °C. Post-treatment with nitric acid at 80 °C.
C-750-Cl	Pyrolysis conducted in a CO <sub>2</sub> atmosphere at 750 °C. Post-treatment with hydrochloric acid.
C-750-P-80	Pyrolysis conducted in a CO <sub>2</sub> atmosphere at 750 °C. Post-treatment with potassium permanganate at 80 °C.
C-750-P	Pyrolysis conducted in a CO <sub>2</sub> atmosphere at 750 °C. Post-treatment with potassium permanganate.
C-600-N	Pyrolysis conducted in a CO <sub>2</sub> atmosphere at 600 °C. Post-treatment with nitric acid.
C-750-N	Pyrolysis conducted in a CO <sub>2</sub> atmosphere at 750 °C. Post-treatment with nitric acid.
C-850-N	Pyrolysis conducted in a CO <sub>2</sub> atmosphere at 850 °C. Post-treatment with nitric acid.

### 2.3. Catalyst Characterization

The catalysts were analysed by different spectroscopic and analytical techniques to determine their physical and chemical properties. X-ray fluorescence (XRF) and elemental analysis were used to determine the material's chemical composition using the equipments AXIOS from Phillips and LECO CHNS-932 analyzer, respectively. The specific surface area of the materials was determined by the Brunauer-Emmett-Teller (BET) method using the Micromeritics ASAP 2020 instrument. The surface chemistry was analysed by Fourier transformed infrared spectroscopy (FTIR) using a Thermo Nicolet Nexus 670. In addition, electron transmission micrographs (TEM) were taken in a JEOL JEM 2100 microscope (80-200 kV, 0.23 mm), joined to an XEDS analysis system (Oxford Inca).

### 2.4. Prednisone removal experiment

Figure 2 shows the diagram of the experimental setup used for the CWAO and adsorption tests. The reactor used is a Parker Autoclave Engineers 100 mL capacity complete mix mini reactor, jacketed for temperature control and agitated by magnetic stirring with a paddle stirrer. The stirring speed was set at 700 rpm to not limit mass transfer. All catalyst experiments were performed at 15 bar pressure with an initial concentration of 20 mg·L<sup>-1</sup> of prednisone in distilled water. The temperature, catalyst dosage and pH were varied to study their effect on the process. The catalysis experiments were carried out at 100 or 170 °C, while the adsorption kinetics experiments were performed at 30 °C. A catalyst dosage of 0.3 g·L<sup>-1</sup> or 1.5 g·L<sup>-1</sup> were used to observe the impact of this variable on the reduction of total organic carbon (TOC). To evaluate the influence of the medium acidity, different initial pH were tested: 3, 5 and 6 (this last corresponds to the natural pH of the dissolution). The adjust of pH was done with HCl.

### 2.5. Analytical methods

Samples were analysed by high-performance chromatography (HPLC, Agilent 1260 series) to follow the concentration of prednisone in each experiment. Each sample was filtered with filters of PTFE of 0.45 μm. The column used was a poroshell 120 of 4.6x150 mm. A mobile phase of 35 % acetonitrile and 65 % water-acetic (17 mM) was used, and the flow rate was 0.7 mL·min<sup>-1</sup>. It was measured at 30 °C and the wavelength was selected at 245 nm. For these conditions, the retention time of prednisone was 4.9 min. The samples' total organic carbon (TOC) was measured in a Shimadzu TOC-VCSH analyzer. The reaction intermediates were determined in by LC-QTOF-MS in a Bruker Impact 2 spectrophotometer. Finally, leached iron was measured by ICP with an

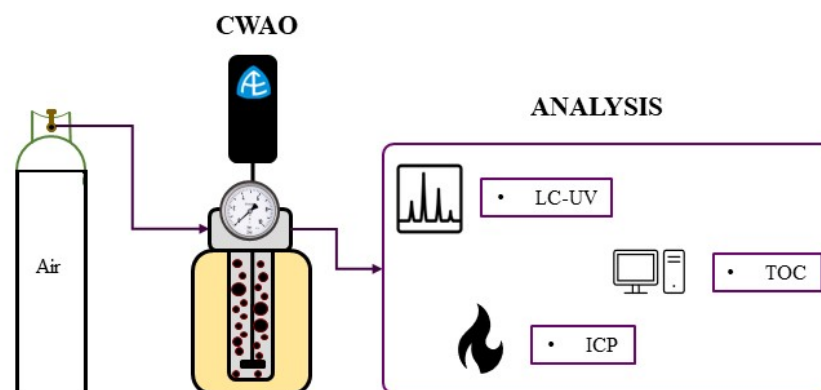


Figure 2: Experimental setup of CWAO and adsorption experiments

SPECTRO Arcos equipment.

### 3. Results and discussion

#### 3.1. Characterization results of the catalysts

##### 3.1.1. Characterization of the sewage sludge

The sewage sludge used initially was thoroughly characterized in a previous study [31], which revealed a high concentration of iron in the sludge. The level of iron in this sample is 14.27% which is a result of the chemicals used in the sedimentation process of water treatment.

##### 3.1.2. Elemental analysis and XRF

The elemental analysis and XRF results of the synthesized materials are presented in Table 2. The effects of pyrolysis atmosphere, temperature and post-treatments on the chemical composition of the catalysts are shown in Table 2.

Table 2 shows that materials synthesised in a  $\text{CO}_2$  atmosphere at temperatures above  $600\text{ }^\circ\text{C}$  have a lower percentage of carbon, while nitrogen atmosphere does not change the carbon percentage. Furthermore, the increase in carbon content in the samples treated with different acids is noteworthy. Similar values of carbon composition have been found in literature, where Tu et al. [6] report a carbon percentage of 25.4% for the sewage sludge after the pyrolysis process, and 43.9% after an acid treatment. This effect is due to the leaching of the metals present in the ashes of the pyrolysed material. Table 2 also shows the reduction in the percentage of Fe, K or P.

Table 2: Elemental analysis and X-ray Fluorescence results of each catalyst.

Elemental content (%)	Sewage Sludge	C-600	N-600	N-750	C-750	C-600-N	C-850-N	C-750-N-80	C-750-N	C-750-Cl	C-750-P-80	C-750-P
C	40.45	33.92	35.44	32.80	26.98	51.76	42.43	50.53	48.72	47.66	21.53	23.16
H	5.05	1.17	1.14	1.01	0.76	1.68	1.53	1.51	1.59	1.41	1.08	1.04
N	6.85	4.32	4.18	2.84	2.42	6.65	2.35	5.23	5.08	4.33	2.07	2.2
S	0.6	0.20	0.18	0.15	0.23	0.30	0.39	0.3	0.28	0.57	0.12	0.18
O	18.13	28.50	27.99	29.98	27.9	25.62	37.37	21.13	19.83	20.91	27.54	27.3
Si	1.92	2.51	2.44	2.65	3.84	3.98	11.38	12.84	11.07	11.41	3.69	3.83
Fe	14.27	14.17	13.76	15.16	19.98	4.09	1.35	4.38	5.04	5.71	19.98	19.43
K	2.14	2.36	2.23	2.47	2.72	0.94	2.35	1.37	1.52	1.92	2.43	2.86
Al	0.76	1.06	1.00	1.06	1.38	0.72	1.33	1.23	1.58	1.76	1.36	1.37
P	5.47	6.17	6.09	6.51	8.09	1.56	0.63	1.19	1.28	1.15	6.35	6.56
Cl	0.64	0.15	0.20	0.10	0.08	0.12	0.01	0.14	0.1	0.86	-	0.02
Ti	0.16	0.15	0.15	0.17	0.22	0.26	0.35	0.56	0.47	0.6	0.22	0.21
Ca	2.64	2.93	2.81	3.15	3.66	0.80	0.22	0.49	0.5	0.46	3.13	3.15
Cu	0.10	0.08	0.08	0.09	0.12	0.07	0.03	0.29	0.27	0.42	0.14	0.16
Mg	0.60	0.93	0.88	0.87	0.85	0.30	0.09	0.12	0.21	0.21	0.63	0.74
Zn	0.10	0.10	0.09	0.09	0.13	0.07	0.03	0.05	0.06	0.2	0.15	0.13
Pb	0.05	0.02	0.02	0.02	0.04	0.07	0.03	0.04	0.05	0.12	0.05	0.04
Cr	0.02	0.02	0.02	0.01	0.03	0.02	0.04	0.05	0.05	0.06	0.02	0.02
Ni	0.01	0.01	0.01	-	0.03	0.02	0.03	0.04	0.04	0.05	0.03	0.03
Zr	-	-	-	-	0.02	-	-	0.02	0.02	-	-	-
Co	-	-	0.04	-	-	-	-	0.01	0.01	-	-	-
Rb	-	-	-	-	0.01	-	-	0.01	0.01	0.01	0.01	0.01
Mn	0.03	0.04	0.02	0.04	0.05	0.01	0.00	0.01	0.01	0.01	9.81	8.34
Sr	0.02	0.02	0.02	0.01	0.03	0.02	0.04	-	0.01	0.01	0.04	0.03
Br	0.01	-	-	-	-	-	-	0.01	0.01	-	-	-

### 3.1.3. Porosity properties

Table 3 shows the specific surface area ( $S_{\text{BET}}$ ), total volume, micropore volume and mesopore volume of the samples synthesised.

Table 3: Textural properties of the prepared catalysts.

Carbon	$S_{\text{BET}}$ ( $\text{m}^2 \cdot \text{g}^{-1}$ )	$V_{\text{T}}$ ( $\text{cm}^3 \cdot \text{g}^{-1}$ )	$V_{\text{micro}}$ ( $\text{cm}^3 \cdot \text{g}^{-1}$ )	$V_{\text{meso}}$ ( $\text{cm}^3 \cdot \text{g}^{-1}$ )	$V_{\text{micro}}/V_{\text{T}}$
N-600	2	0.012	0.000	0.011	0.016
C-600	1	0.012	0.000	0.012	0.016
N-750	11	0.021	0.000	0.021	0.022
C-750	131	0.144	0.030	0.144	0.207
C-750-N-80	387	0.455	0.089	0.367	0.194
C-750-Cl	300	0.401	0.062	0.339	0.154
C-750-P-80	147	0.126	0.034	0.092	0.267
C-750-P	133	0.124	0.032	0.092	0.258
C-600-N	168	0.200	0.033	0.168	0.164
C-750-N	372	0.430	0.087	0.344	0.202
C-850-N	420	0.650	0.091	0.566	0.139

The role of the pyrolysis atmosphere becomes significant in the material surface development at temperatures exceeding 600 °C. Table 3 shows that C-600 and N-600, materials synthesised in  $\text{CO}_2$  and  $\text{N}_2$  atmospheres respectively, have a similar specific surface area. However, as the temperature increases to 750 °C, the difference becomes substantial, 11 to 131  $\text{m}^2 \cdot \text{g}^{-1}$  for N-750 and C-750, respectively. The increase in porosity is primarily reflected in the increase in mesoporosity, which is almost seven times greater for C-750 compared to N-750.

It is appreciable in Table 3 a positive correlation with temperature pyrolysis and specific surface area. For samples C-700-N, C-750-N and C-850-N it is shown that the pyrolysis temperature significantly increases the surface development of the samples from 168 to 372 to 420  $\text{m}^2 \cdot \text{g}^{-1}$ . We observed that longer times of reaction, higher temperature or more gas flow in the pyrolysis process are essential to control the specific surface area of the materials obtained [32]. Above 750 °C, the ratio of micropores to the total pore volume of the material decreases with increasing temperature, although the volume of mesopores and micropores increases.

The post-treatment is crucial for the development of the specific surface area. Acid washing has a significant positive effect on this parameter. This effect can be attributed to the leaching of metals from the ash contained in the material, as shown in Table 2. This lends to support that the inorganic part of the material is non-porous and does not allow the development of this parameter [33]. The treatments that implies permanganate do not change the specific surface area.

### 3.1.4. Surface chemistry analysis

To analyse the effect of  $\text{CO}_2$  on the carbon surface, the surface chemistry of the material is examined at different temperatures. Figure 3 show the FTIR analysis of each material synthesised at 600 and 750 °C in  $\text{CO}_2$  and  $\text{N}_2$  atmospheres.

All samples exhibit the same functional groups, but the intensity is significantly higher at 750 °C in a  $\text{CO}_2$  atmosphere. Analysing the bands, the peak at 3048  $\text{cm}^{-1}$  corresponds to the vibration of the -OH bonds, while the 1541  $\text{cm}^{-1}$  band is associated with the -CO-NH groups [1]. The peak at 1080  $\text{cm}^{-1}$  is related to the silicon coupling in the material's structure, corresponding to the vibration of the Si-O-C bonds. Many authors identify this band as carbon associated with silicon [34, 35].

As can be seen in Figure 3, the increase in pyrolysis temperature causes an increased proportion of O-based functional groups on the char surface. These results support that above 600 °C,  $\text{CO}_2$  (the activating agent) is crucial for the development of the specific surface area and the surface chemistry [34].

Figure 3 shows an increase in oxygenated groups on the catalyst surface as the pyrolysis temperature increases. This effect is attributed to the reaction of  $\text{CO}_2$  with the carbonaceous component of the sewage sludge. The  $\text{CO}_2$  activation involved partial gasification reaction between carbon (C) and carbon dioxide ( $\text{CO}_2$ ),

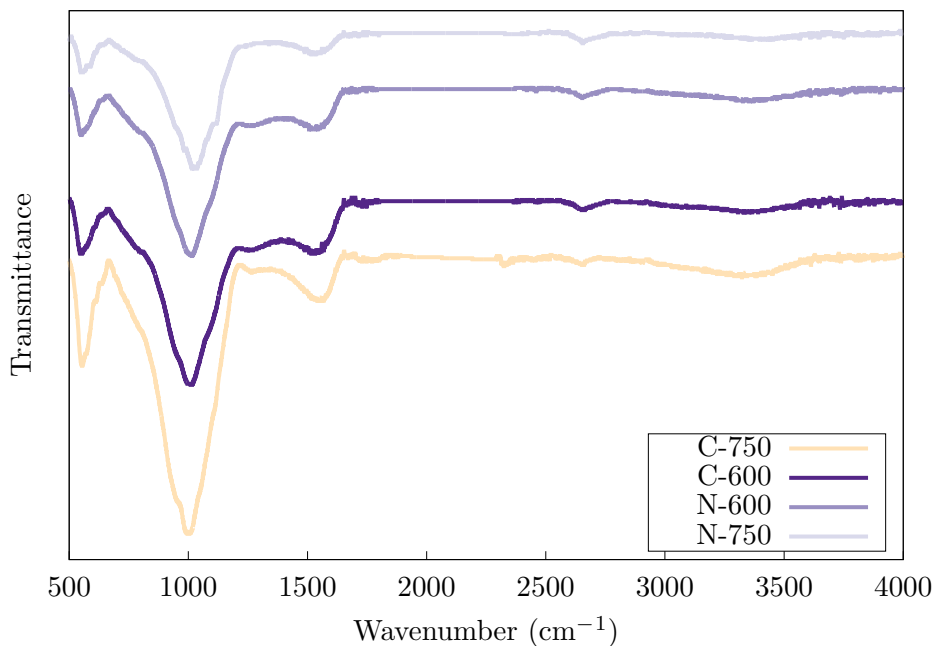


Figure 3: FTIR spectra of the carbonaceous materials synthesised under different atmospheres and temperatures.

resulting in an endothermic reaction represented by reaction 1, which presents an activation energy of 173  $\text{KJ}\cdot\text{mol}^{-1}$  [36]:



When pyrolyzing at 600 °C, the temperature is insufficient to initiate the reaction. Consequently, the porosity, composition (by elemental analysis) and FTIR spectra for N-600 and C-600 catalysts. However, 750 °C is sufficient to enhance the porosity of the solid material due to the reaction 1, resulting in a reduction in the proportion of carbon in C-750 compared to the catalysts prepared at lower pyrolysis temperature or with a different atmosphere, C-600, N-600 and N-750 (Table 2). The increase in porosity is also a consequence of this reaction, with higher values for samples C-750, C-750-N and C-850-N compared to those synthesised at 600°C and/or  $\text{N}_2$  atmosphere.

Macro-level analysis of  $\text{CO}_2$  activation indicated that the  $\text{CO}_2$  activation proceeds through: hole-throughing, hole-making, and hole-enlargement [37]. At 600 °C, the active sites on the surface of the raw material were limited to a small percentage of the specific surface area, therefore, the activation proceeds slowly [36]. Finally, the effects of the post-treatments on the surface chemistry of the material are shown in Figure 4.

Figure 4 show the changes in the surface chemistry of the treated catalysts with a post-treatment. The increase of -OH bonds after treatments with  $\text{HNO}_3$  and  $\text{KMnO}_4$  at 80 °C is noteworthy. Both processes ( $\text{HNO}_3$  and  $\text{KMnO}_4$ ) greatly favour the formation of these groups on the catalyst surface. Treatments with the same agents at room temperature generate these radicals at a lower rate. The peak at 1541  $\text{cm}^{-1}$  is favoured by acid treatments, as also observed by Yu et al. [38] in the synthesis of their catalysts. However, the permanganate treatment does not modify this peak, possibly because the inorganic fraction is not leached. Furthermore, the peak at 1080  $\text{cm}^{-1}$  becomes more prominent with each acid wash. This could be attributed to the rise in carbon content in the material, resulting in an increase in Si-O-C single bonds. Finally, the 675  $\text{cm}^{-1}$  peak corresponds to the Si-O-Fe vibration [1], and interestingly this band disappears after the acid-washes.

### 3.1.5. TEM characterization

TEM analysis was performed to investigate the morphological properties of catalysts after each post-treatment. Several micrographs were taken at different magnifications, in different areas of each catalyst. Despite the presence of metals evidenced by XRF (Table 2), only a few metallic particles were found, suggesting that the metals must be integrated in the catalysts' structure or as very small metallic particles. Figure 5 shows TEM images obtained for each material. XEDS analysis of the solid particles and their composition can be consulted on the Supplementary material (Figures S1-S6, Tables S2-S6).

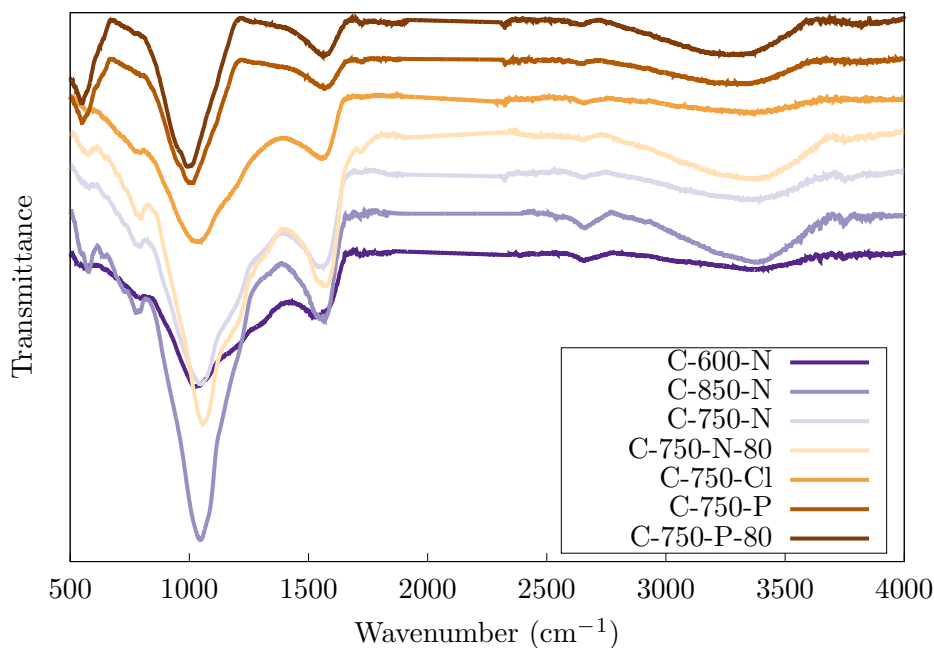


Figure 4: FTIR spectra of the carbonaceous materials synthesised with different post-treatments.

Figures 5a and 5b shows the catalyst C-750 at different magnifications. An important amount of Fe is detected by XEDS, in good agreement with XRF results, where a high concentration of silicon, aluminum and iron were found.

Figures 5c to 5j show the catalysts after post-treatment. The application of acid treatments (HCl, HNO<sub>3</sub> or HNO<sub>3</sub> at 80 °C) impact on the morphology of the solid and its composition (Figures S3, S4 and S5, Tables S4, S5 and S6). The solid particles seem to exhibit a homogeneous structure, resulting from the creation of voids previously occupied by the inorganic metallic fraction. Figure 5c, 5e and 5g show a solid particle of C-750-N-80, C-750-N and C-750-Cl catalyst, and a closer view can be seen in figure 5d, 5f and 5h, were no metallic particles are observed, pointing to the more homogeneously and better distributed inorganic fraction in the catalysts. XEDS spectra show significantly lower peaks related to all the major metallic components. However, iron still represents a notable percentage of this fraction, as detailed in tables S4, S5 and S6.

On the other hand, permanganate treatment with or without temperature do not change the chemical and textural properties of the material. Figures 5i and 5j show TEM images of these materials. XEDS analysis are presented in Figures S6 and S7, were a good correlation with XRF results is observed.

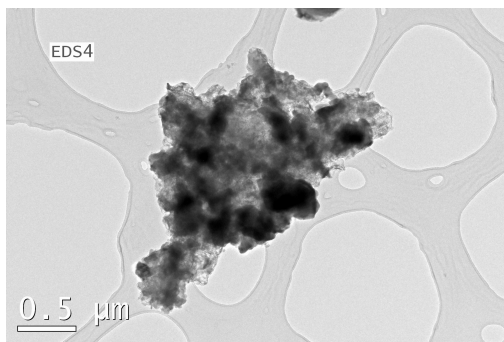
Finally, Figure S8 illustrate a specific type of particle observed in all the samples, which is mainly based on silicon and aluminium, indicating that they are impurities introduced during the wastewater treatment process.

## 3.2. Catalytic activity

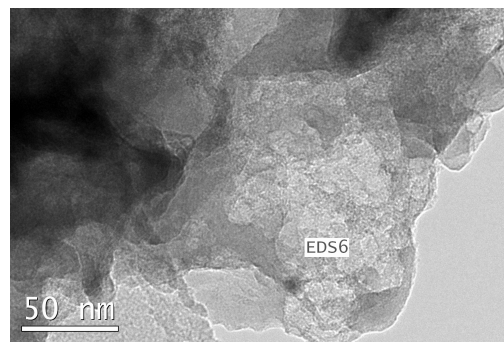
### 3.2.1. Effect of pyrolysis atmosphere

To determine the effect of the pyrolysis atmosphere at 600 and 750 °C on prednisone removal, a set of catalysis experiments were carried out. Figure 6 shows the evolution of prednisone concentration over time, comparing the catalyst (CWAO) and non-catalyst (WAO) experiments.

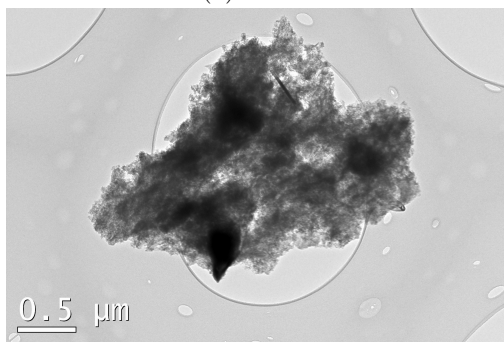
Figure 6 shows a clear difference between the experiment with (CWAO) and without catalyst (WAO), indicating that these materials promote -OH radicals which enhance the conversion of prednisone. Increasing the pyrolysis temperature also improves the catalysis, with N-750 and C-750 showing faster conversions than N-600 and C-600. The observed increase in the kinetics of the process may be attributed to the increase in mesoporosity in the materials obtained with a pyrolysis temperature of 750 °C. This increase in mesoporosity facilitates the entry of prednisone molecules into the active centres of the catalyst. In addition, CO<sub>2</sub> atmosphere during pyrolysis gave a better performance on the catalysis. The high catalytic activity of C-750 is attributed



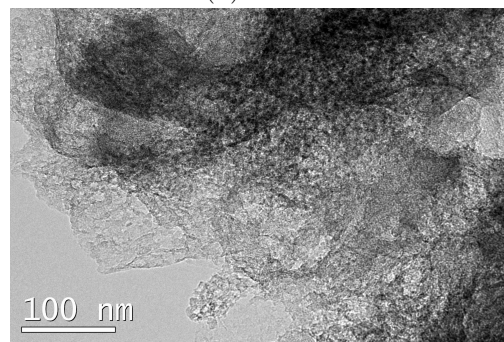
(a) C-750



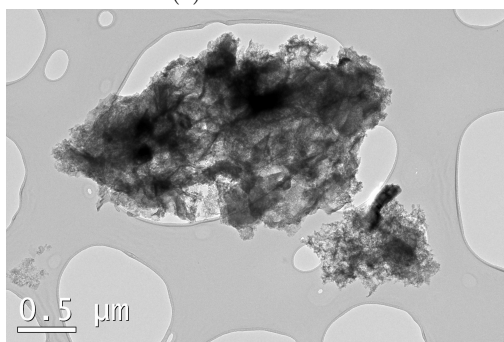
(b) C-750



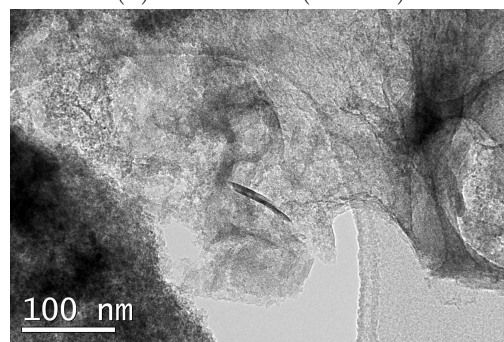
(c) C-750-N-80



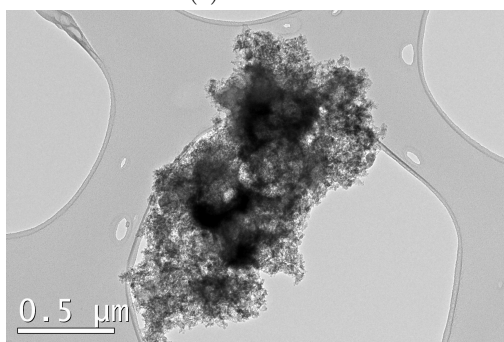
(d) C-750-N-80 (100 nm)



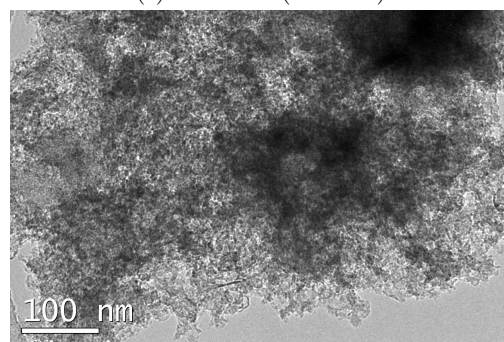
(e) C-750-N



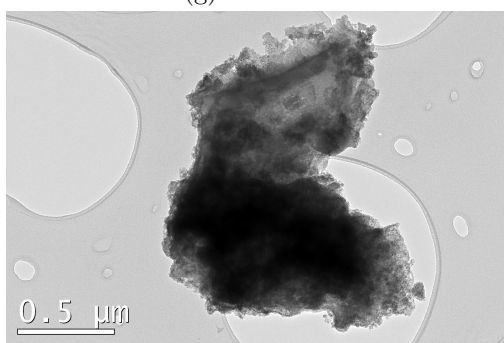
(f) C-750-N (100 nm)



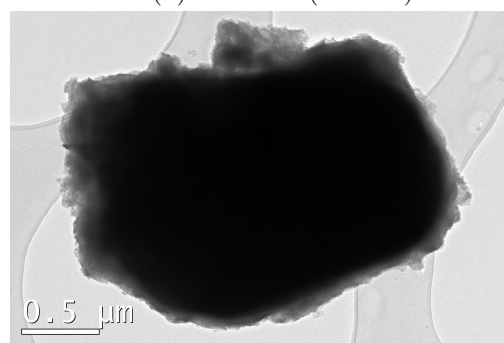
(g) C-750-Cl



(h) C-750-Cl (100 nm)



(i) C-750-P



(j) C-750-P-80

Figure 5: TEM images of each catalyst.

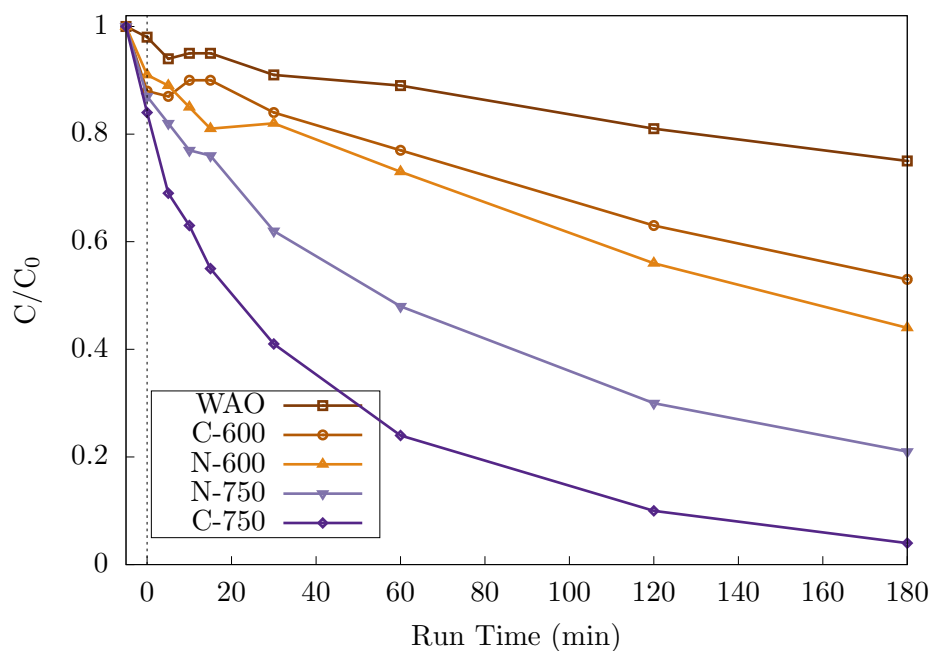


Figure 6: Evolution of prednisone concentration with time during CWAO with the SDC's synthesised at different atmospheres and temperatures:  $D_{\text{cat}}=0.3 \text{ g}\cdot\text{L}^{-1}$ ,  $T=100 \text{ }^\circ\text{C}$ ,  $P=15 \text{ bar}$ .

to its higher specific surface area, resulting from the  $\text{CO}_2$  reaction during pyrolysis, as shown in Figure 3. Based on these results, further experiments were carried out with materials synthesised in a  $\text{CO}_2$  atmosphere. The influence of the pyrolysis temperature and different post-treatments on the catalysis were studied.

### 3.2.2. Effect of pyrolysis temperature

Figure 7 displays the influence of the pyrolysis temperature on the removal of prednisone through CWAO.

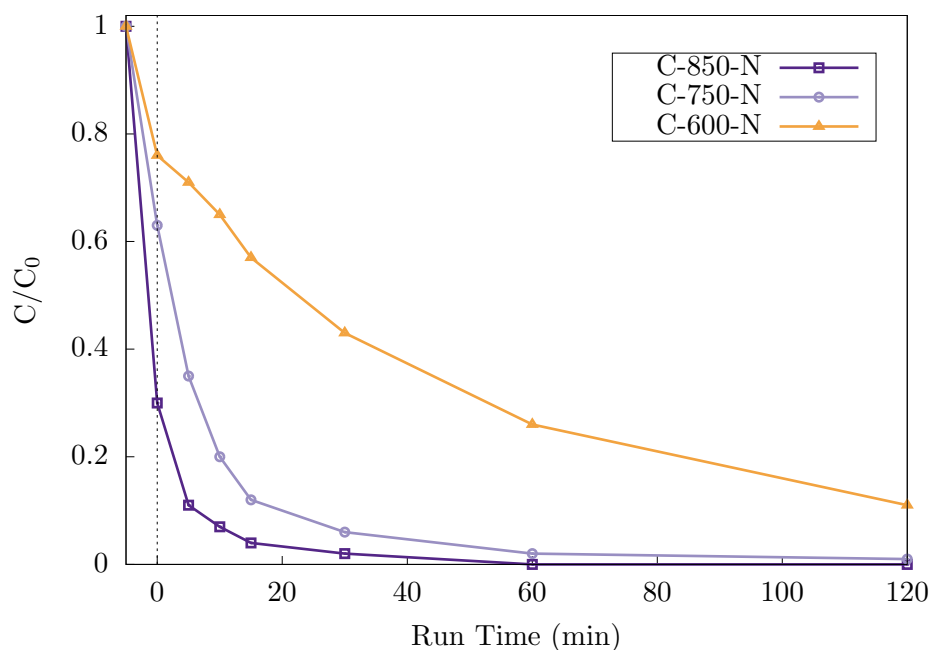


Figure 7: Evolution of prednisone concentration with time during CWAO with SDC's synthesised at different pyrolysis temperatures:  $D_{\text{cat}} = 0.3 \text{ g}\cdot\text{L}^{-1}$ ,  $T = 100 \text{ }^\circ\text{C}$ ,  $P = 15 \text{ bar}$ .

Figure 7 illustrates the catalytic effect of SBCs synthesised at  $\text{CO}_2$  atmosphere and different pyrolysis tem-

peratures. There is a significant positive correlation with temperature pyrolysis and the adsorption properties, effect observed on the high removal of the pollutant at time zero. At temperatures higher than 800 °C, CO<sub>2</sub> opens the material's pores, improving the contaminants' adsorption [32, 35, 37]. Other authors have also reported increase porosity with pyrolysis temperature. Sierra et al. [35] present data on carbonaceous adsorbents produced by pyrolysis at temperatures of 600 and 900 °C, with subsequent acid post-treatment, showing porosity values of 260 to 600 m<sup>2</sup>.g<sup>-1</sup>, respectively.

The porosity of the material plays an essential role in the process. A notable enhancement in the kinetic of prednisone degradation over time is observed for the C-750-N (94.2% for 30 mins) catalyst compared to the C-600-N (52.7% for 30 mins) catalyst. This increase is associated with the BET surface area of both catalysts, 372 m<sup>2</sup>.g<sup>-1</sup> and 168 m<sup>2</sup>.g<sup>-1</sup>, respectively (Table 3), illustrating the significance of the pyrolysis temperature in both, catalytic and/or adsorption processes.

Further tests were carried out with a pyrolysis temperature of 750 °C because treatment at 600 °C did not result in significant improvement, even with a post-pyrolysis step. At a time of 30 minutes, the catalyst synthesised at 600 °C showed a 57.3% conversion of the compound, which is considerably lower than the conversions achieved by catalysts C-750-N and C-850-N. Conversely, the increase of the adsorption capacity is of not interest.

### 3.2.3. Effect of post-treatment

The degradation of prednisone by CWAO with the sewage sludge derived catalysts with different post-treatments is shown in Figure 8.

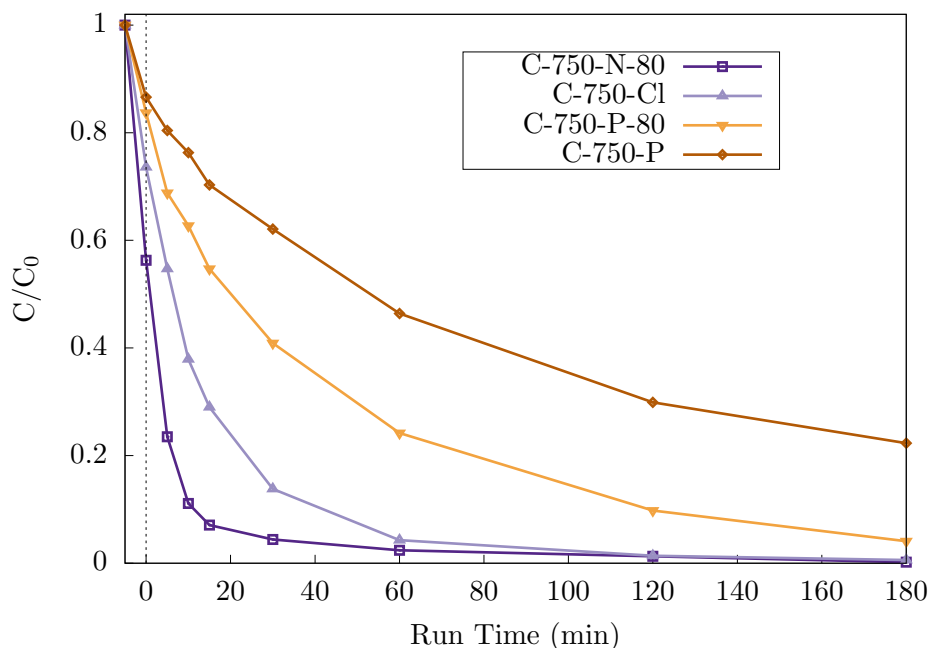


Figure 8: Evolution of prednisone concentration with time during CWAO with the SDC:  $D_{cat}=0.3$  g.L<sup>-1</sup>, T=100 °C, P=15 bar.

These results highlight the importance of specific surface area development for the CWAO process, corroborated by Marques et al. [29]. The material with no post-treatment C-750 (Figure 6) exhibits good removal of the pollutant. A comparable method of synthesis has previously been tested for the treatment of phenolic waters [39]. In this study, SBCs were obtained using CO<sub>2</sub> and had a specific surface area of 169.1 m<sup>2</sup>.g<sup>-1</sup>, resulting in a 60% phenol conversion rate. All post-treatments that imply an acid wash favoured the pollutants' removal, due to the porosity development as shown in Table 3. Figure 8 show a faster removal of prednisone with C-750-N-80, C-750-N and C-750-Cl, obtaining values of conversion of 95.6%, 94.24% and 86.15% at 30 minutes of the process, respectively. Similarly, the materials experienced a significant increase in specific surface area, as shown in Table 3. On the other hand, permanganate treatments, disfavour the catalytic activity of the synthesised char. This treatment only promote the addition of -OH groups as we can see in Figure 4 where the band which correspond to -OH bonds has a remarkable increase. This hindered of catalysis may be due to the

repulsion of prednisone and its by-products to the active centers of the material.

The results indicate that the characteristics of the solid, specifically the functional groups and porosity, have a significant influence on the oxidation of prednisone. The increase in specific surface area is attributed to the leaching of metals. In addition, the increase in porosity favours the catalysis process by facilitating the access of the prednisone molecules to the active sites. Nevertheless, despite the leaching of metals by acid treatment, a significant proportion of metals remains in the structure of the material (Table 2). On the other hand, it is important to note that the carbonaceous matrix can generate electrons, supporting the oxidation-reduction reactions. Numerous metal-free catalysts have been used in CWAO processes, with graphene being a particularly noteworthy example [40].

### 3.2.4. Effect of pH

In order to evaluate the influence of pH on the performance of the process a set of experiments was conducted at various pH levels using no post-treatment catalyst (C-750). The experiments were conducted under acidic conditions to investigate the impact of acidification on catalysis. This is because, as shown in Figure 8, acid washing enhances the catalytic properties of the material. Therefore, it would be worthwhile to compare the effects of acidification on the medium. The results are shown in Figure 9.

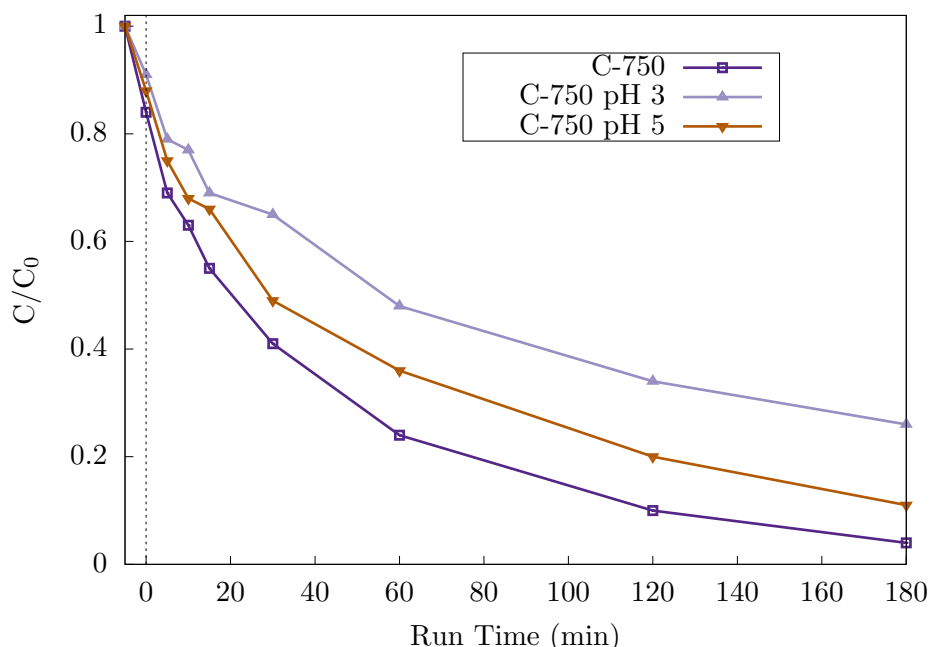


Figure 9: Evolution of prednisone concentration with time during pH experiments for C-750 catalyst:  $D_{\text{cat}}=0.3 \text{ g}\cdot\text{L}^{-1}$ ,  $T=100 \text{ }^\circ\text{C}$ ,  $P=15 \text{ bar}$ .

The initial pH value is an important factor to consider. According to Figure 9, decreasing pH to 3 and 5 disfavour the catalytic process compared to the natural pH medium (pH 6). Several authors have observed this effect with different systems, catalysts and pollutants. For example for degradation of p-nitrophenol over a Ru or Pt catalysts [41], showing an increase in the reaction rate as the pH increases from 9 to 22  $\text{mol}_{\text{PNP}}\cdot\text{mol}_{\text{Ru}}^{-1}\cdot\text{h}^{-1}$ . This effect can be explained by differentiating between azo and non-azo compounds. The oxidation of non-azo compounds increases with higher values of pH, effect observed for prednisone. The opposite effect would occur for azo compounds [42]. The oxidation of prednisone is associated with the adsorption of the pollutant on the surface of the catalyst. In the case of azo compounds, there exists an opposite charge between the catalyst surface and the intermediates, leading to more effective adsorption of pollutants [42].

### 3.2.5. Adsorption-Catalyst experiments

Figure 10 compare prednisone removal by adsorption and CWAO. These graphs allow for the evaluation of the relationship between the adsorptive and catalytic properties of each material. In addition, Figure 11 displays

the comparative results for the TOC reduction.

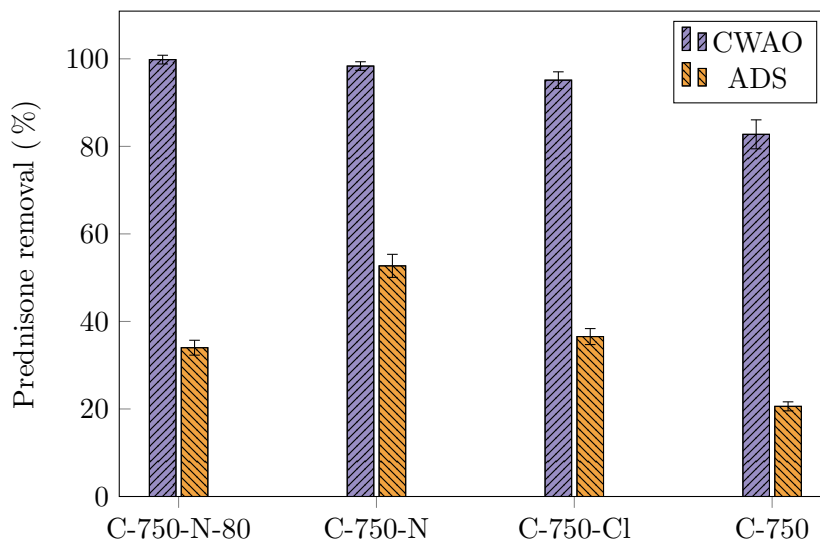


Figure 10: Prednisone removal for the adsorption ( $T= 30\text{ }^{\circ}\text{C}$ ,  $D_{\text{cat}}= 0.3\text{ g}\cdot\text{L}^{-1}$ ,  $P= \text{atm}$ ) and CWAO ( $T= 100\text{ }^{\circ}\text{C}$ ,  $D_{\text{cat}}= 0.3\text{ g}\cdot\text{L}^{-1}$ ,  $P= 15\text{ bar}$ ) experiments.

The material with the best adsorption properties is C-750-N, followed by C-750-Cl, C-750-N-80 and C-750. The sequence is ordered not only by the specific surface area but also by the influence of the surface chemistry of the sample on prednisone. An increase in -OH groups in the material disfavours the performance of the adsorption process. This is evident in the case of C-750-N-80, with a higher amount of -OH groups (Figure 4). In addition, this effect is also reflected in Figure 11, where the reduction of TOC by the C-750-N-80 catalyst is lower than the reduction by the C-750-N and C-750-Cl catalysts. Despite having the highest specific surface area, this material does not possess good adsorption properties. Finally, although the unwashed material (C-750) is a poor adsorbent, it exhibits good catalytic properties.

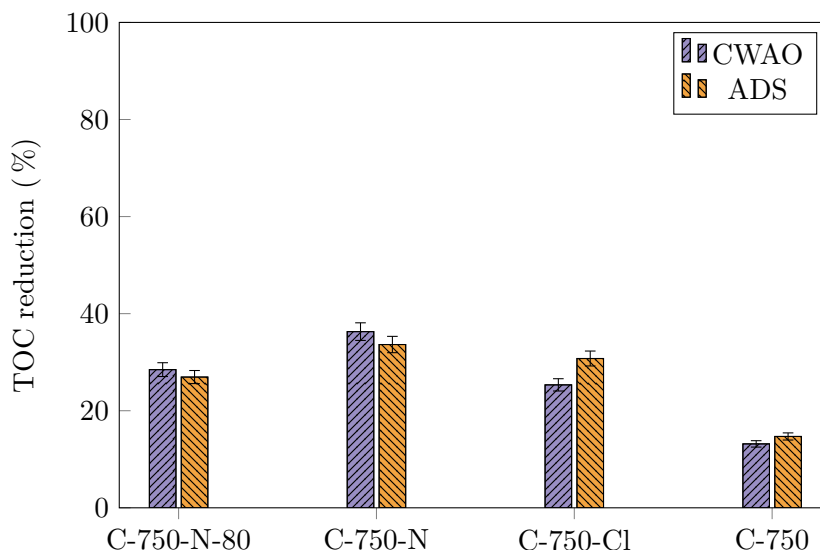


Figure 11: TOC reduction for the adsorption ( $T= 30\text{ }^{\circ}\text{C}$ ,  $D_{\text{cat}}= 0.3\text{ g}\cdot\text{L}^{-1}$ ,  $P= \text{atm}$ ) and CWAO ( $T= 100\text{ }^{\circ}\text{C}$ ,  $D_{\text{cat}}= 0.3\text{ g}\cdot\text{L}^{-1}$ ,  $P= 15\text{ bar}$ ) experiments.

The C-750-Cl and C-750 catalysts exhibit a higher TOC reduction value for the adsorption experiment compared to the catalysis experiment. Conversely, the nitric-treated catalysts show the opposite effect. This can be attributed to the disfavoured effect of temperature in the adsorption. Furthermore, since these values are very similar, it can be concluded that at the experimental temperature of  $100\text{ }^{\circ}\text{C}$ , the compound has barely mineralised, despite the complete conversion of the pollutant.

### 3.2.6. Effect of temperature and dosage of catalyst

Figures 12 and 13 show, respectively, the elimination of TOC by CWAO and the values of inorganic carbon (IC) obtained after three hours. The CWAO experiments were performed under different temperature and dosage of catalyst, presenting the results obtained when intensifying the operating conditions. Figure 13 illustrates the capacity of each catalyst to mineralize prednisone, demonstrating that the increase of catalyst dosage, a higher degree of mineralization is obtained.

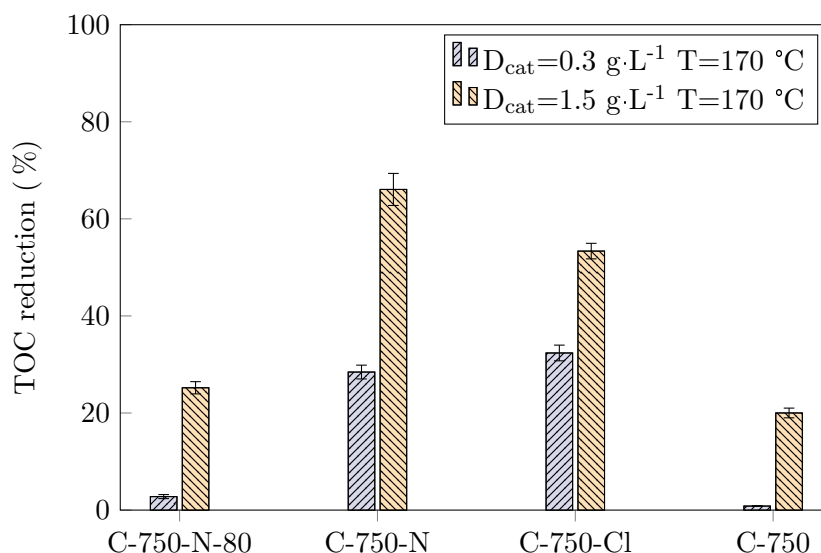


Figure 12: Reduction of prednisone TOC at higher temperature and dosage of catalyst.

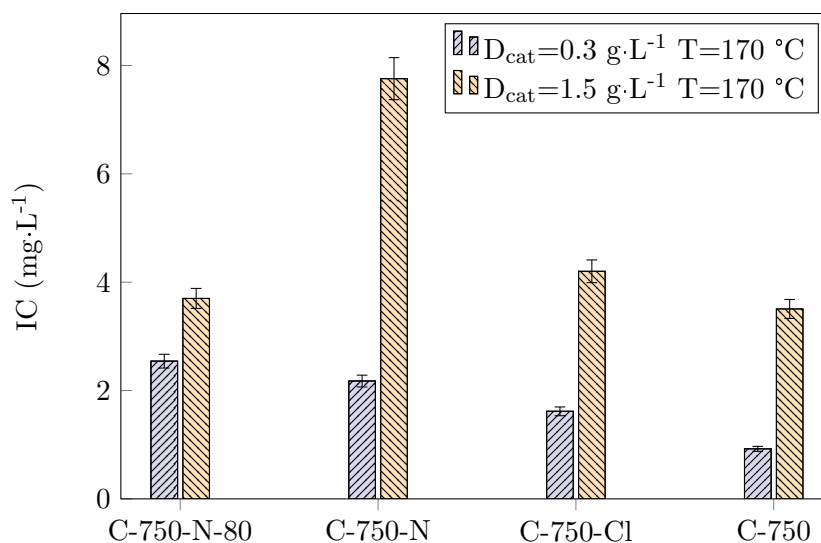


Figure 13: IC values of the treated effluent at higher temperature and higher dosage of catalyst.

In the analysis of the results, it is noteworthy that the experiments carried out with a catalyst dosage of  $0.3 \text{ g}\cdot\text{L}^{-1}$  and a temperature of  $170 \text{ }^\circ\text{C}$  resulted in a decrease of the total organic carbon for all the catalysts in comparison with the adsorption experiment. This effect demonstrates the influence of temperature in adsorption of prednisone and its byproducts. However,  $0.3 \text{ g}\cdot\text{L}^{-1}$  of catalyst is not enough for a high mineralization of the pollutant. The most remarkable decrease is for the sample C-750-N-80. For this catalyst the percentage of TOC reduction decreased from 28.46 % to 2.78 % (Figure 12). A comparison between C-750-N-80 and C-750 shows that TOC reduction and IC are similar. This finding supports the significance of surface chemistry. Despite having three times the specific surface area, sample C-750-N-80 did not yield the expected results as the other samples washed with acid. It is important to have strategies to introduce functional groups that favour catalysis, such as strongly acidic groups or electron-giving groups like amines or carboxylic groups [43]. The process can be significantly improved by increasing the catalyst dosage. This leads to higher TOC reduction values

and increased IC generation in all experiments. The catalyst C-750-N produces the highest value, followed by C-750-Cl. Increasing the catalyst dosage improves the oxidation of pollutants by providing more active sites and surface area for organic compounds to react with oxygen [44].

### 3.2.7. Leaching of Fe

The stability of the iron contained in the catalysts was analysed. The concentration of iron in the effluent from the experiments carried out at 170 °C and 1.5 g·L<sup>-1</sup> was measured by ICP. The results obtained are shown in Table 4.

Table 4: Metal leaching measured after 3 h of reaction: P = 15 bar, T=170 °C, D<sub>cat</sub> = 1.5 g·L<sup>-1</sup>.

Carbon	Fe (mg·L <sup>-1</sup> )
C-750-N-80	0.081 ± 0.009
C-750-N	< 0.015
C-750-Cl	< 0.015
C-750	< 0.015

Table 4 shows that there was no detectable iron leaching in any of the tests performed, except for C-750-N-80 which showed some iron leaching above the instrumentation limit. The reason for the high leaching resistance was that the small iron particles interacted with the carbonaceous support, greatly improving catalyst stability and leaching resistance (See EDS spectrums in Figures S2-S8). Other authors have obtained similar results. For example Marques et al. [29] obtained with a SBC synthesized by pyrolysis under CO<sub>2</sub> atmosphere the lowest iron leachate in the process of CWAO. Additionally, Mohedano et al. [45] did not observe any leachate from his SBC, even when working at 80 °C and pH 3 in a CWPO process.

### 3.2.8. Catalyst stability and reusability

The lifetime of the catalyst is an important factor in CWAO process. Several consecutive catalytic cycles were carried out with the C-750-N catalyst to observe its stability and reusability. The experiments were conducted at 100°C, 15 bar and a catalyst dose of 0.3 g·L<sup>-1</sup>. The reactor was cooled at the end of the reaction time, and a new 20 mg·L<sup>-1</sup> solution of prednisone was added with the same catalyst already used. Figure 14 shows the time evolution of the prednisone concentration for three consecutive runs.

The results demonstrate the reusability of the catalyst for the degradation of prednisone. After 120 min, almost complete removal of the initial prednisone was obtained in the first and second runs. And about 90 % was removed after the third run. The difference could be due to the loss of catalyst during the sample taken. Nevertheless, the highly oxidizing environment during the reaction could be modifying the catalyst surface chemistry, being necessary to perform additional studies to identify possible reasons for catalyst deactivation.

## 4. Degradation by-products of prednisone. Reaction mechanism

With the aim of identifying the intermediate compounds formed during the CWAO reaction, samples at 90 min and 180 min were analyzed by (+)-ESI-LC-MS, comparing the results with a pattern prednisone solution of 20 mg·L<sup>-1</sup>. Positive-mode operation allowed us to see the prednisone ion in the pattern solution with a retention time of 1.80 min, where the highest intensity was obtained ((+)-ESI m/z = 359.1862; see Figure S1 in the Supporting Information). According to the molecular formula calculated from the accurate mass and MS fragmentation, the structural formulas of the main degradation products were proposed. The retention times and compositions of molecular ions TP1-TP6 are shown in Table S1.

The ·OH reacted with organic pollutants by H-abstraction, addition and electron-transfer. The single electron transfer of ·OH was commonly in electron-rich organic compounds, such as phenol, toluene, aniline, and hexamethylbenzene. In the prednisone degradation mechanism depicted in Figure 15, three degradation pathways have been proposed. Pathway A is the simultaneous oxidation of prednisone molecule from both sides. Pathway B can be initiated by electrophilic reactions attacking the electron-rich parts of organic compounds. In the case of prednisone, this leads to the cleavage of the double bond. In addition, the compound (m/z = 311.1875) originates from the loss of the alcohol group preferentially due to dehydration that often occurs in

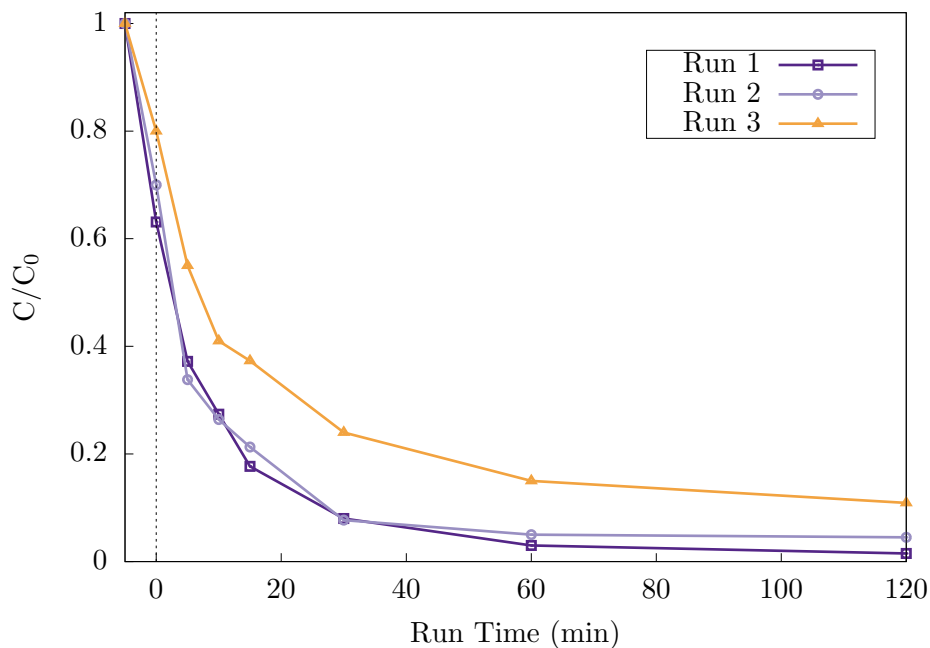


Figure 14: Reusability of C-750-N catalyst for prednisone degradation after three consecutive cycles.

AOP processes [46]. Dealkylation of the alcohol chain can also occur, which, together with oxidation of the alkyl chains, is the predominant pathway when AOPs are applied [47]. In addition, the compound ( $m/z = 290.9062$ ) has also reduced the ketone group, as occurred in the degradation route proposed by Pérez-Estrada et al. [48], who degraded 4-methylamino antipyrine under solar AOPs. The demethylation of the previous compound generates the compound ( $m/z = 274.2762$ ). Dealkylation is common in AOPs; in fact, Frontistis et al. [49] reported dealkylation as the main oxidation mechanism in the  $17\alpha$ -ethyl estradiol degradation pathway under UV/ $H_2O_2$  process. Finally, pathway C begins with the oxidation of cyclopentanic part of the molecule, leading to the formation of products with  $m/z$  345, depending on whether the cyclohexanic part of the molecule adjacent to cyclopentanic is cleaved or remains intact; subsequent oxidation of both fragments leads to the formation of other products.

## 5. Conclusions

Sewage sludge-based carbons can be used as catalysts for the removal of prednisone in CWAO processes. Synthesis at  $750\text{ }^\circ\text{C}$  and  $CO_2$  atmosphere offers a material with good catalytic properties. Treatments with different acids have been tested, improving the catalytic activity due to porosity development in all cases. Treatments involving nitric acid at  $80\text{ }^\circ\text{C}$ , nitric acid at ambient temperature and hydrochloric acid at ambient temperature have increased the specific surface area from  $131\text{ m}^2\cdot\text{g}^{-1}$  to  $387$  (C-750-N-80),  $372$  (C-750-N) and  $300\text{ m}^2\cdot\text{g}^{-1}$  (C-750-Cl). In addition, pyrolysis temperature can also enhance specific surface area to  $420\text{ m}^2\cdot\text{g}^{-1}$  (C-850-N). The effect of the surface chemistry have also been studied, finding that the introduction of -OH groups on the catalyst surface disfavors the compound's degradation and its mineralization. The catalyst C-750-N have shown the best performance, exhibiting a full conversion of prednisone by CWAO, and achieving an adsorption value of  $52.7\%$ . The increase of temperature favours the oxidation process, reaching a maximum TOC reduction of  $66\%$  after 3 hours of the process. In addition, no iron leaching occurred throughout the process. Therefore, our catalysts developed in the present study not only outperform in terms of performance, but can also demonstrate such catalytic activity at operating conditions and feedstock costs in the removal of emerging pollutants such as prednisone.

## 6. Acknowledgements

This work has been supported by the MICINN through the CATAD3.0 project PID2020-116478RB-I00. In addition, the authors acknowledge funding from the Comunidad de Madrid (Spain), through the REMTAVARES Network (S2018/EMT-4341).

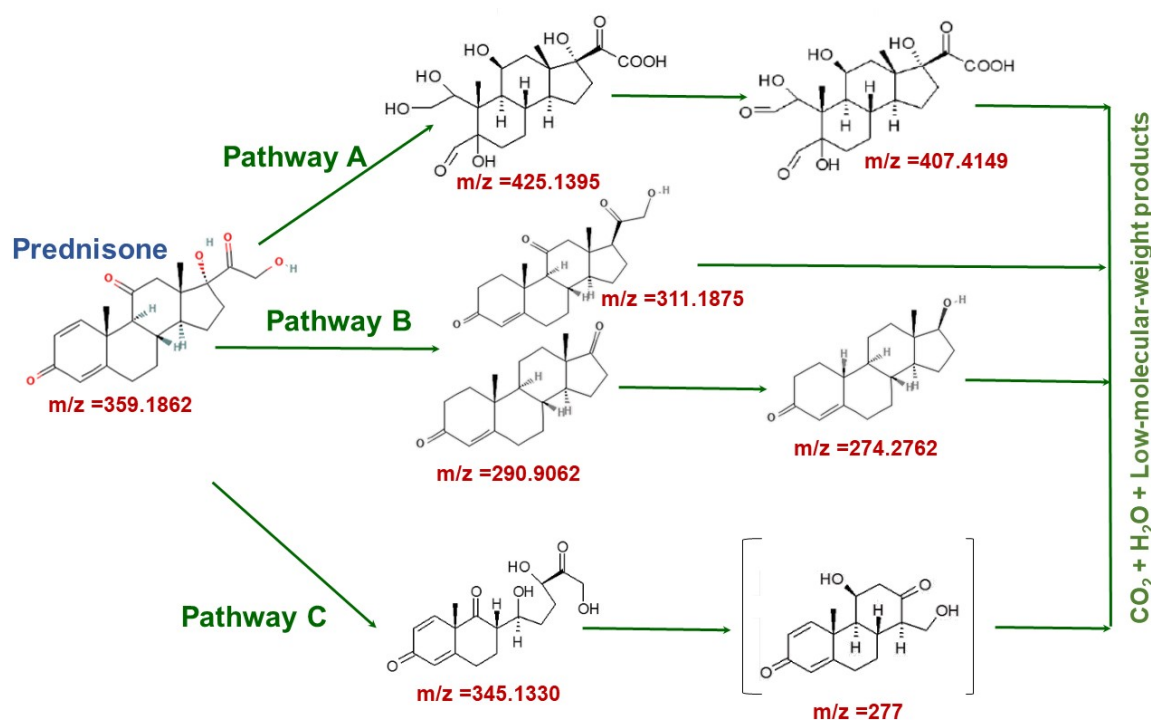


Figure 15: Proposed pathway of prednisone degradation in CWAO process.

## References

- (1) Yuan, S. J.; Dai, X. H. Facile synthesis of sewage sludge-derived mesoporous material as an efficient and stable heterogeneous catalyst for photo-Fenton reaction. *Applied Catalysis B: Environmental* **2014**, *154-155*, 252–258, DOI: 10.1016/j.apcatb.2014.02.031.
- (2) Bandosz, T. J.; Block, K. Effect of pyrolysis temperature and time on catalytic performance of sewage sludge/industrial sludge-based composite adsorbents. *Applied Catalysis B: Environmental* **2006**, *67*, 77–85, DOI: 10.1016/j.apcatb.2006.04.006.
- (3) Kim, J. H.; Oh, J. I.; Lee, J.; Kwon, E. E. Valorization of sewage sludge via a pyrolytic platform using carbon dioxide as a reactive gas medium. *Energy* **2019**, *179*, 163–172, DOI: 10.1016/j.energy.2019.05.020.
- (4) Li, G.; Chai, S.; Zhang, G.; Liu, J.; Zhang, Y.; Lv, Y.; Wang, Y.; Zhao, Y. Deactivation characteristics of Ce-modified Cu-based carbon materials for catalytic wet air oxidation of phenol wastewater. *Journal of Environmental Chemical Engineering* **2022**, *10*, 108228, DOI: 10.1016/j.jece.2022.108228.
- (5) Stüber, F.; Polaert, I.; Delmas, H.; Font, J.; Fortuny, A.; Fabregat, A. Catalytic wet air oxidation of phenol using active carbon: performance of discontinuous and continuous reactors: Catalytic wet air oxidation of phenol using active carbon. *Journal of Chemical Technology & Biotechnology* **2001**, *76*, 743–751, DOI: 10.1002/jctb.441.
- (6) Tu, Y.; Xiong, Y.; Tian, S.; Kong, L.; Descorme, C. Catalytic wet air oxidation of 2-chlorophenol over sewage sludge-derived carbon-based catalysts. *Journal of Hazardous Materials* **2014**, *276*, 88–96, DOI: 10.1016/j.jhazmat.2014.05.024.
- (7) Mian, M. M.; Liu, G.; Fu, B. Conversion of sewage sludge into environmental catalyst and microbial fuel cell electrode material: A review. *Science of The Total Environment* **2019**, *666*, 525–539, DOI: 10.1016/j.scitotenv.2019.02.200.
- (8) Yu, L.; Liu, Y.; Wei, H. A review: preparation of sludge derived carbons and their performance in wastewater treatment. *Desalination and water treatment* **2020**, *201*, 169–182, DOI: 10.5004/dwt.2020.26146.

- (9) Agrafioti, E.; Bouras, G.; Kalderis, D.; Diamadopoulos, E. Biochar production by sewage sludge pyrolysis. *Journal of Analytical and Applied Pyrolysis* **2013**, *101*, 72–78, DOI: 10.1016/j.jaap.2013.02.010.
- (10) Gavrilescu, M.; Demnerová, K.; Aamand, J.; Agathos, S.; Fava, F. Emerging pollutants in the environment: present and future challenges in biomonitoring, ecological risks and bioremediation. *New Biotechnology* **2015**, *32*, 147–156, DOI: 10.1016/j.nbt.2014.01.001.
- (11) Moreno Ríos, A. L.; Gutierrez-Suarez, K.; Carmona, Z.; Ramos, C. G.; Silva Oliveira, L. F. Pharmaceuticals as emerging pollutants: Case naproxen an overview. *Chemosphere* **2022**, *291*, 132822, DOI: 10.1016/j.chemosphere.2021.132822.
- (12) Garcia-Costa, A. L.; Alves, A.; Madeira, L. M.; Santos, M. S. Oxidation processes for cytostatic drugs elimination in aqueous phase: A critical review. *Journal of Environmental Chemical Engineering* **2021**, *9*, 104709, DOI: 10.1016/j.jece.2020.104709.
- (13) Hamon, P.; Moulin, P.; Ercolei, L.; Marrot, B. Oncological ward wastewater treatment by membrane bioreactor: Acclimation feasibility and pharmaceuticals removal performances. *Journal of Water Process Engineering* **2018**, *21*, 9–26, DOI: 10.1016/j.jwpe.2017.11.012.
- (14) Yin, K.; He, Q.; Liu, C.; Deng, Y.; Wei, Y.; Chen, S.; Liu, T.; Luo, S. Prednisolone degradation by UV/chlorine process: Influence factors, transformation products and mechanism. *Chemosphere* **2018**, *212*, 56–66, DOI: 10.1016/j.chemosphere.2018.08.032.
- (15) McNeil, P. L.; Nebot, C.; Sloman, K. A. Physiological and Behavioral Effects of Exposure to Environmentally Relevant Concentrations of Prednisolone During Zebrafish ( *Danio rerio* ) Embryogenesis. *Environmental Science & Technology* **2016**, *50*, 5294–5304, DOI: 10.1021/acs.est.6b00276.
- (16) Franquet-Griell, H.; Gómez-Canela, C.; Ventura, F.; Lacorte, S. Anticancer drugs: Consumption trends in Spain, prediction of environmental concentrations and potential risks. *Environmental Pollution* **2017**, *229*, 505–515, DOI: 10.1016/j.envpol.2017.06.011.
- (17) Schriks, M.; Van Leerdam, J. A.; Van Der Linden, S. C.; Van Der Burg, B.; Van Wezel, A. P.; De Voogt, P. High-Resolution Mass Spectrometric Identification and Quantification of Glucocorticoid Compounds in Various Wastewaters in The Netherlands. *Environmental Science & Technology* **2010**, *44*, 4766–4774, DOI: 10.1021/es100013x.
- (18) Liu, Z.; Zhang, F. S.; Wu, J. Characterization and application of chars produced from pinewood pyrolysis and hydrothermal treatment. *Fuel* **2010**, *89*, 510–514, DOI: 10.1016/j.fuel.2009.08.042.
- (19) Munirasu, S.; Haija, M. A.; Banat, F. Use of membrane technology for oil field and refinery produced water treatment—A review. *Process Safety and Environmental Protection* **2016**, *100*, 183–202, DOI: 10.1016/j.psep.2016.01.010.
- (20) Mahanty, B.; Ansari, S. A.; Mohapatra, P. K.; Leoncini, A.; Huskens, J.; Verboom, W. Liquid-liquid extraction and facilitated transport of f-elements using an N-pivot tripodal ligand. *Journal of Hazardous Materials* **2018**, *347*, 478–485, DOI: 10.1016/j.jhazmat.2017.12.068.
- (21) Roy, S.; Vashishtha, M. Catalytic Wet Air Oxidation of Oxalic Acid using Platinum Catalysts in Bubble Column Reactor: A Review. *Journal of Engineering Science and Technology Review* **2010**, *3*, 95–107, DOI: 10.25103/jestr.031.17.
- (22) Marrone, P. A. Supercritical water oxidation—Current status of full-scale commercial activity for waste destruction. *The Journal of Supercritical Fluids* **2013**, *79*, 283–288, DOI: 10.1016/j.supflu.2012.12.020.
- (23) Baloyi, S.; Moma, J. Catalytic wet air oxidation of phenol by cordierite honeycomb washcoated with Al/Zr pillared bentonite in a plug flow reactor. *Journal of Environmental Chemical Engineering* **2020**, *8*, 104186, DOI: 10.1016/j.jece.2020.104186.
- (24) Baloyi, J.; Ntho, T.; Moma, J. Synthesis of highly active and stable Al/Zr pillared clay as catalyst for catalytic wet oxidation of phenol. *Journal of Porous Materials* **2019**, *26*, 583–597, DOI: 10.1007/s10934-018-0667-3.

- (25) Wang, H.; Lu, Y.; Han, Y.; Lu, C.; Wan, H.; Xu, Z.; Zheng, S. Enhanced catalytic toluene oxidation by interaction between copper oxide and manganese oxide in Cu-O-Mn/-Al<sub>2</sub>O<sub>3</sub> catalysts. *Applied Surface Science* **2017**, *420*, 260–266, DOI: 10.1016/j.apsusc.2017.05.133.
- (26) Gosu, V.; Dhakar, A.; Sikarwar, P.; Kumar, U. A.; Subbaramaiah, V.; Zhang, T. C. Wet peroxidation of resorcinol catalyzed by copper impregnated granular activated carbon. *Journal of Environmental Management* **2018**, *223*, 825–833, DOI: 10.1016/j.jenvman.2018.06.093.
- (27) Gutiérrez-Sánchez, P.; Álvarez Torrellas, S.; Larriba, M.; Gil, M. V.; Garrido-Zoido, J. M.; García, J. Efficient removal of antibiotic ciprofloxacin by catalytic wet air oxidation using sewage sludge-based catalysts: Degradation mechanism by DFT studies. *Journal of Environmental Chemical Engineering* **2023**, *11*, 109344, DOI: 10.1016/j.jece.2023.109344.
- (28) Yu, Y.; Wei, H.; Yu, L.; Gu, B.; Li, X.; Rong, X.; Zhao, Y.; Chen, L.; Sun, C. Catalytic wet air oxidation of m-cresol over a surface-modified sewage sludge-derived carbonaceous catalyst. *Catalysis Science & Technology* **2016**, *6*, 1085–1093, DOI: 10.1039/C5CY00900F.
- (29) Marques, R. R. N.; Font, J.; Fortuny, A.; Bengoa, C.; Fabregat, A.; Stuber, F. Performance of Sludge Based Activated Carbons in Catalytic Wet Air Oxidation of Phenol. *International Journal of Chemical Reactor Engineering* **2010**, *8*, DOI: 10.2202/1542-6580.2165.
- (30) Stüber, F.; Smith, K.; Mendoza, M. B.; Marques, R.; Fabregat, A.; Bengoa, C.; Font, J.; Fortuny, A.; Pullket, S.; Fowler, G.; Graham, N. Sewage sludge based carbons for catalytic wet air oxidation of phenolic compounds in batch and trickle bed reactors. *Applied Catalysis B: Environmental* **2011**, *110*, 81–89, DOI: 10.1016/j.apcatb.2011.08.029.
- (31) Sanz-Santos, E.; Álvarez Torrellas, S.; Larriba, M.; Calleja-Cascajero, D.; García, J. Enhanced removal of neonicotinoid pesticides present in the Decision 2018/840/EU by new sewage sludge-based carbon materials. *Journal of Environmental Management* **2022**, *313*, 115020, DOI: 10.1016/j.jenvman.2022.115020.
- (32) Ahmadpour, A.; Do, D. D. The preparation of active carbons from coal by chemical and physical activation. *Carbon* **1996**, *34*, 471–479.
- (33) Zou, J.; Dai, Y.; Wang, X.; Ren, Z.; Tian, C.; Pan, K.; Li, S.; Abuobeidah, M.; Fu, H. Structure and adsorption properties of sewage sludge-derived carbon with removal of inorganic impurities and high porosity. *Bioresource Technology* **2013**, *142*, 209–217, DOI: 10.1016/j.biortech.2013.04.064.
- (34) Jindarom, C.; Meeyoo, V.; Kitiyanan, B.; Rirksomboon, T.; Rangsunvigit, P. Surface characterization and dye adsorptive capacities of char obtained from pyrolysis/gasification of sewage sludge. *Chemical Engineering Journal* **2007**, *133*, 239–246, DOI: 10.1016/j.cej.2007.02.002.
- (35) Sierra, I.; Iriarte-Velasco, U.; Cepeda, E. A.; Gamero, M.; Aguayo, A. T. Preparation of carbon-based adsorbents from the pyrolysis of sewage sludge with CO<sub>2</sub>. Investigation of the acid washing procedure. *Desalination and Water Treatment* **2016**, *57*, 16053–16065, DOI: 10.1080/19443994.2015.1075428.
- (36) Nomura, K.; Terwilliger, P. Self-dual Leonard pairs. *Special Matrices* **2019**, *7*, 1–19, DOI: 10.1515/spma-2019-0001.
- (37) Rodríguez-Reinoso, F.; Molina-Sabio, M. Activated carbons from lignocellulosic materials by chemical and/or physical activation: an overview. *Carbon* **1992**, *30*, 1111–1118, DOI: 10.1016/0008-6223(92)90143-K.
- (38) Yu, Y.; Wei, H.; Yu, L.; Zhang, T.; Wang, S.; Li, X.; Wang, J.; Sun, C. Surface modification of sewage sludge derived carbonaceous catalyst for m-cresol catalytic wet peroxide oxidation and degradation mechanism. *RSC Advances* **2015**, *5*, 41867–41876, DOI: 10.1039/C5RA00858A.
- (39) Marques, R.; Stüber, F.; Smith, K.; Fabregat, A.; Bengoa, C.; Font, J.; Fortuny, A.; Pullket, S.; Fowler, G.; Graham, N. Sewage sludge based catalysts for catalytic wet air oxidation of phenol: Preparation, characterisation and catalytic performance. *Applied Catalysis B: Environmental* **2011**, *101*, 306–316, DOI: 10.1016/j.apcatb.2010.09.033.

- (40) Raquel P. Rocha Manuel Fernando R. Pereira, J. L. F. Metal-free carbon materials as catalysts for wet air oxidation. *Catalysis Today* **2020**, *356*, 189196, DOI: 10.1016/j.cattod.2019.04.047.
- (41) Martín-Hernández, M.; Carrera, J.; Suárez-Ojeda, M. E.; Besson, M.; Descorme, C. Catalytic wet air oxidation of a high strength p-nitrophenol wastewater over Ru and Pt catalysts: Influence of the reaction conditions on biodegradability enhancement. *Applied Catalysis B: Environmental* **2012**, *123-124*, 141–150, DOI: 10.1016/j.apcatb.2012.04.001.
- (42) Sushma; Kumari, M.; Saroha, A. K. Performance of various catalysts on treatment of refractory pollutants in industrial wastewater by catalytic wet air oxidation: A review. *Journal of Environmental Management* **2018**, *228*, 169–188, DOI: 10.1016/j.jenvman.2018.09.003.
- (43) Restivo, J.; Rocha, R. P.; Silva, A. M.; Órfão, J. J.; Pereira, M. F.; Figueiredo, J. L. Catalytic performance of heteroatom-modified carbon nanotubes in advanced oxidation processes. *Chinese Journal of Catalysis* **2014**, *35*, 896–905, DOI: 10.1016/S1872-2067(14)60103-0.
- (44) Santiago, A; Sousa, J; Guedes, R; Jeronimo, C; Benachour, M Kinetic and wet oxidation of phenol catalyzed by non-promoted and potassium-promoted manganese/cerium oxide. *Journal of Hazardous Materials* **2006**, *138*, 325–330, DOI: 10.1016/j.jhazmat.2006.05.118.
- (45) Mohedano, A.; Monsalvo, V.; Bedia, J.; Lopez, J.; Rodriguez, J. Highly stable iron catalysts from sewage sludge for CWPO. *Journal of Environmental Chemical Engineering* **2014**, *2*, 2359–2364, DOI: 10.1016/j.jece.2014.01.021.
- (46) Liu, Y.; He, X.; Duan, X.; Fu, Y.; Fatta-Kassinos, D.; Dionysiou, D. Significant role of UV and carbonate radical on the degradation of oxytetracycline in UV-AOPs: Kinetics and mechanism. *Water Research* **2016**, *95*, 195204, DOI: 10.1016/j.watres.2016.03.011.
- (47) Acero, J. L.; Stremmler, K.; von Gunten, U. Degradation kinetics of atrazine and its degradation products with ozone and OH radicals: a predictive tool for drinking water treatment. *Environ. Sci. Technol* **2000**, *34*, 591597, DOI: 10.1016/j.watres.2016.03.011.
- (48) Pérez-Estrada, L.; Malato, S.; Agüera, A.; Fernández-Alba, A. R. Degradation of dipyrone and its main intermediates by solar AOPs. *Catalysis Today* **2007**, *129*, 207214, DOI: 10.1016/j.cattod.2007.08.008.
- (49) Frontistis, Z.; Kouramanos, M.; Moraitis, S.; Chatzisyneon, E.; Hapeshi, E.; Fatta-Kassinos, D.; Xekoukoulotakis, N. P.; Mantzavinos, D. UV and simulated solar photodegradation of 17-ethynylestradiol in secondary-treated wastewater by hydrogen peroxide or iron addition. *Catalysis Today* **2015**, *252*, 8492, DOI: 10.1016/j.cattod.2014.10.012.